

A redox-based model for carbonate platform drowning and Ocean Anoxic Events

B.P. Smith¹, C. Kerans², W.W. Fischer¹,

¹Division of Geological and Planetary Sciences, California Institute of Technology, Pasadena, California
91125, USA

²Department of Geological Sciences, Jackson School of Geosciences, University of Texas at Austin, Austin,
Texas 78712, USA

Key Points:

- A model for carbonate platform drowning was developed based on changing patterns of carbonate production and dissolution.
- Ocean anoxia reduces both carbonate dissolution and the amount of carbonate overproduction in the surface oceans.
- Linking carbonate chemistry to ocean redox conditions allowed slower sedimentation over long (10^5 - 10^6 year) timescales.

Corresponding author: Ben Smith, bpsmith@caltech.edu

This article has been accepted for publication and undergone full peer review but has not been through the copyediting, typesetting, pagination and proofreading process, which may lead to differences between this version and the [Version of Record](#). Please cite this article as [doi: 10.1029/2021GL093048](https://doi.org/10.1029/2021GL093048).

This article is protected by copyright. All rights reserved.

Abstract

The deposition of marine carbonate rocks is influenced by climate and seawater chemistry. Carbonate platforms usually keep pace with subsidence and sea level rise but platform drowning occurs when carbonate sedimentation slows or when siliciclastics replace carbonates. Identifying specific mechanism(s) behind platform drowning is critical for understanding global environmental changes such as Ocean Anoxic Events (OAES).

We developed a model for OAES which couples ocean basin redox processes to rates of carbonate sedimentation. Well-oxygenated oceans have steep gradients in saturation state such that deep-ocean dissolution is balanced by carbonate overproduction in shallow water. Through anaerobic metabolisms, deep-ocean anoxia reduces both dissolution and overproduction, leading to slower accumulation rates in shallow-water environments. This quasi-steady state response links carbonate sedimentation with longer timescales associated with redox changes. Redox-based drowning may have acted alongside other mechanisms to create spatially diverse patterns of platform drowning during Mesozoic OAES and other Phanerozoic hyperthermal events.

Plain Language Summary

Carbonate minerals precipitate from ions dissolved in water. Thick packages of carbonate rocks often form in shallow, tropical waters, and their accumulation rate depends on the availability of ions as well as biological agents that catalyze carbonate deposition such as animals and microbes. Geologic patterns in carbonate rocks are sensitive to these controls on accumulation rates, tying them to Earth's surface chemistry and ecosystems.

Sometimes chemical changes in the oceans cause far-reaching effects that influence patterns observed in carbonate rocks. During the Mesozoic Era, episodes of lowered dissolved oxygen in the world's oceans often coincided with a phenomenon known as platform drowning. Platform drowning occurs when carbonate platforms of carbonate deposition like the modern Bahamian Islands experienced slower sedimentation rates and sank into deeper water. Interestingly, there are several chemical pathways that could cause platform drowning, and unraveling the underlying drivers is key for understanding the nature of past environmental changes. Here we present a concept for platform drowning that emphasizes the role of microbes and their effects on global ocean chemistry. This idea helps explain the long timescales of platform drowning and may explain similar patterns during other low-oxygen episodes in Earth's past.

1 Introduction

Carbonate sediments are the largest (by mass) physical products of Earth's biogeochemical cycles. Consequently, changes in the rates, modes, and mechanisms of carbonate precipitation often accompany major carbon cycle perturbations such as Snowball Earth episodes (Hoffman et al., 1998, 2017), the end-Permian extinction (Baud et al., 2007; Kelley et al., 2020; Lehrmann et al., 2015), and the Paleocene-Eocene Thermal Maximum (PETM) (Penman et al., 2016; Zachos et al., 2005). Several well-known examples occur in strata spanning Ocean Anoxic Events (OAES)—a series of carbon cycle changes that perturbed Mesozoic climate and the redox structure of marine basins (Arthur et al., 1987; Jenkyns, 2010; Schlanger & Jenkyns, 1976; Scholle & Arthur, 1980). In shallow-water carbonates, OAES are marked by carbonate platform 'drowning' in which deeper, organic-rich deposits displaced shallow-water facies (Arthur & Schlanger, 1979; Schlager, 1981; Phelps et al., 2015) (Fig. 1a). Schlager (1981) christened this pattern as the 'paradox of drowned platforms' because growth rates in modern carbonates exceed all but the fastest rates of sea level rise. Hallock and Schlager (1986) provided an initial solution that invoked reduced sedimentation rates, and subsequent research has focused on chemical and biological mechanisms that hinder carbonate growth. Such mechanisms are valu-

64 able for understanding the nature of environmental changes at OAEs because they might
65 provide a common factor linking geochemical records, platform drowning, and biotic turnover
66 among calcifying organisms (Föllmi et al., 1994; Kiessling & Simpson, 2011; Krencker
67 et al., 2020; Phelps et al., 2015; Trecalli et al., 2012).

68 OAEs are complex events in which a single cause—commonly thought to be a rapid
69 injection of volcanic CO₂—triggers a cascade of related events that could lead to plat-
70 form drowning (Jenkyns, 2010). However, anoxic conditions rarely impinge upon shallow-
71 water environments because waves efficiently mix atmospheric oxygen into the water col-
72 umn (Beatty et al., 2008), and so many models of platform drowning focus on indirect
73 linkages to deep-basin anoxia. Early work by Hallock and Schlager (1986) pointed to dis-
74 solved nutrients as possible causal drowning agents because many photosymbiotic reef-
75 builders are adapted to low nutrient conditions and thrive in clear, non-turbid seawa-
76 ter. Under this hypothesis, elevated nutrient fluxes drown platforms by stimulating pri-
77 mary production, decreasing light penetration and allowing fleshy non-calcifiers to out-
78 compete the prolific carbonate producers. Such a drowning mechanism is attractive be-
79 cause increased nutrients and primary productivity are also used to explain geochem-
80 ical proxies for redox and weathering (Blättler et al., 2011; Jenkyns, 2010; Lechler et al.,
81 2015). However, excess nutrients may simply shift carbonate sedimentation towards non-
82 skeletal components (e.g., ooids and microbialites) which can comprise a significant por-
83 tion of platform sediments near OAEs (Ettinger et al., 2020; Huck et al., 2010; Krencker
84 et al., 2020). Nutrient-related drowning also implies that non-skeletal carbonates accu-
85 mulate more slowly than the facies they replace, which may not be universally true given
86 high rates of microbial reef production elsewhere in the Phanerozoic record (e.g., Franceschi
87 et al., 2016).

88 Another plausible and popular mechanism for reduced carbonate production near
89 OAEs is ocean acidification (Kiessling & Simpson, 2011) (Fig. 1b). By analogy to an-
90 thropogenic climate change, volcanic CO₂ invades the surface oceans over short timescales,
91 causing a drop in pH and the saturation states of calcite and aragonite (Zeebe & Wolf-
92 Gladrow, 2001); this drop in pH is ultimately mitigated over 10 ky timescales due to
93 seafloor carbonate dissolution and associated carbonate compensation processes (Archer
94 et al., 1997). While acidification has been invoked for many carbon cycle perturbations,
95 there are several issues with implicating it as the sole driver of platform drowning. First,
96 Earth's carbon cycle has a negative feedback which negates ocean acidification over timescales
97 longer than 10 ky (Hönisch et al., 2012; Knoll et al., 2011). In contrast, many platform
98 drowning events and intervals of biotic turnover occur over intervals exceeding 100 ky.
99 Second, carbon is well-mixed on millennial timescales such that the onset of ocean acid-
100 ification should be synchronous, yet stratigraphic records for OAEs vary through both
101 time and space (Heldt et al., 2010)(Fig. 1a). Together these factors suggest that addi-
102 tional processes were also important in developing the patterns observed in platform drown-
103 ing associated with OAEs.

104 A third mechanism for platform drowning can be drawn from microbial metabolisms
105 in the carbon cycle, which link Earth's large-scale redox and acid-base cycles (Reinhard
106 & Fischer, 2019). We termed this the 'redox-drowning hypothesis'. While some of these
107 metabolic pathways have long been incorporated into models of ocean-atmosphere chem-
108 istry (e.g., Lasaga et al., 1985), a growing number of studies have begun to explicitly con-
109 sider their effects on sedimentary carbonates (Bergmann et al., 2013; Higgins et al., 2009;
110 Tziperman et al., 2011; Reinhard & Fischer, 2019). In general, anaerobic respiration path-
111 ways produce alkalinity that locally increases the carbonate saturation state of seawa-
112 ter and shallow pore fluids. As such, many studies focus on anoxia as a possible driver
113 of enhanced carbonate precipitation (Grotzinger & Knoll, 1995). However, a small sub-
114 set of studies has instead considered the role of anaerobic metabolisms in setting alkali-
115 nity gradients in the ocean. In this framework, anaerobic metabolisms buffer the deep
116 ocean against dissolution at the expense of oversaturation in surface waters (Higgins et

117 al., 2009; Knoll et al., 2011) (Fig. 1c). Although these studies mostly dealt with the long-
 118 term evolution of ocean redox budgets, Higgins et al. (2009) suggested that similar con-
 119 cepts could be used to interpret patterns in carbonate sedimentation during Phanero-
 120 zoic carbon cycle perturbations such as OAEs. Here we built a simple biogeochemical
 121 carbonate sedimentation flux model to understand how carbonate platform drowning can
 122 be instigated by gradients in inorganic carbon and alkalinity driven by the biological pump
 123 under different redox conditions. We used this model to simulate the onset and dissipa-
 124 tion of ocean anoxia by varying the ratio of alkalinity to dissolved inorganic carbon (DIC)
 125 produced during microbial respiration. Our results indicated that widespread onset of
 126 sulfate reduction within the shallow pore fluids and water column of marine basins would
 127 slow carbonate overproduction in shallow water environments and thereby shift the lo-
 128 cus of carbonate deposition away from the surface oceans, resulting in platform drown-
 129 ing over geological timescales.

130 2 Background

131 2.1 Carbonate production and dissolution in the marine basins

132 The formation of carbonate rocks is the primary sink by which the products of weath-
 133 ering, especially inorganic carbon and alkalinity, are removed from natural waters and
 134 seawater. Over geologic timescales, seawater achieves a sort of quasi-steady state in which
 135 the outgassing and weathering fluxes of inorganic carbon and alkalinity is balanced by
 136 the formation of carbonate rocks in net (Walker et al., 1981; Archer et al., 1997):

$$F_{weathering} = F_{burial} \quad (1)$$

137 A naive interpretation of Eqn. 1 is that the surface oceans produce exactly as much car-
 138 bonate as it needs to balance the alkalinity budget imposed by weathering. In fact, mod-
 139 ern oceans produce carbonate minerals at a rate that is four times higher than weath-
 140 ering inputs (Broecker & Peng, 1982; Sarmiento & Gruber, 2006; Sigman & Boyle, 2000).
 141 This ‘overproduction’ of carbonate is compensated by carbonate dissolution within deep
 142 ocean basins and shallow oxic porewaters more broadly (Walter & Burton, 1990; Broecker,
 143 1998; Laya et al., 2021; Melim et al., 2002):

$$F_{weathering} = F_{prod} - F_{diss} = F_{burial} \quad (2)$$

144 While Eqns. 1 and 2 are equivalent, the latter hints shows that there exist a spec-
 145 trum of possible combinations of precipitation/dissolution that satisfy the geological steady
 146 state condition. While a number of studies have investigated how carbonate chemistry
 147 and production responds to changes in weathering fluxes (e.g., Zeebe & Westbroek, 2003;
 148 Reinhard & Fischer, 2019), Higgins et al. (2009) considered the special case of a fixed
 149 weathering flux ($F_{weathering}$). Under this scenario, a steady state characterized by re-
 150 duced rates of carbonate dissolution would be balanced by reduced carbonate (over)production
 151 in the surface ocean, with a potential corollary of lower carbonate saturation states in
 152 surface seawater.

153 A reasonable question, then, is what factors drove patterns of precipitation and dis-
 154 solution in the past. Carbonate dissolution in the modern ocean is governed by several
 155 factors. Some carbonate dissolves at depth because carbonate minerals are more solu-
 156 ble at low temperatures and high pressures (Zeebe & Wolf-Gladrow, 2001), but this in-
 157 organic effect is comparatively small and a substantial amount of dissolution is driven
 158 by aerobic respiration of organic matter, both in the water column and within sedimen-
 159 tary pore fluids (Archer, 1996; Dunne et al., 2012; Hales, 2003; Laya et al., 2021). Biologically-
 160 driven dissolution is widespread in the modern oceans because oxygenated bottom wa-
 161 ters overlie >95% of the seafloor (Helly & Levin, 2004). However, a myriad of geolog-
 162 ical observations have indicated that marine dioxygen was not as ubiquitous in the past,

and oceans characterized by high rates of anaerobic respiration experienced less dissolution or even net precipitation in porewaters and deeper parts of marine basins (Bergmann et al., 2013; Higgins et al., 2009; Knoll et al., 2016). Following Eqn. 2, a switch to more anaerobic conditions (less dissolution) in the deep oceans during OAEs could reduce carbonate production in the surface ocean because shallow-water sedimentation rate tracks local surface chemistry, rather than the global burial rate. Thus re-organizing patterns of precipitation and dissolution in the ocean may lead to slower local accumulation rates in platforms even if anoxia does not directly impinge on those shallow water settings.

2.2 OAEs and the extent of ocean anoxia

Testing the redox-drowning hypothesis for OAEs requires quantitative data on the extent of ocean anoxia—and ideally the carbon fluxes through aerobic and anaerobic metabolisms. Mass-balance studies of redox-sensitive elements can, in principle, provide such constraints, typically rendered as a percentage of the seafloor overlain by anoxic conditions. However it is useful to note that hindcasting the degree of ancient anoxia still carries uncertainties, and such estimates vary substantially by proxy and material during the same event. For example, the maximum extent of seafloor anoxia during OAE 2 was calculated as 1-2% from $\delta^{238}\text{U}$ in shales (Montoya-Pino et al., 2010), 8-15% from $\delta^{238}\text{U}$ in carbonates (Clarkson et al., 2018), and 40% from $\epsilon^{205}\text{Tl}$ in shales (Ostrander et al., 2017). However, trace element proxies have different oxygen thresholds for drawdown and enrichment, so percentages calculated from different proxies may not be interchangeable (Clarkson et al., 2018).

Another estimate for the extent of anoxia comes from biomarkers derived from specific groups of sulfur-oxidizing anoxygenic photoautotrophs (*Chlorobiaceae*) (Forster et al., 2008; Kuypers et al., 2002; Pancost et al., 2004). These aromatic carotenoid biomarkers track water-column euxinia and they are important marine redox proxies because they indicate that free H_2S was both present and sufficiently abundant within the photic zone (Damsté & Köster, 1998). For OAE 2, biogeochemical paleoceanographic models calibrated to biomarker data estimated that at least 50% of the seafloor was anoxic during peak OAE conditions (Monteiro et al., 2012). Biomarker observations are particularly useful as they provide direct evidence that the $\text{H}_2\text{S}/\text{SO}_4$ redox pair played an expanded role in photosynthesis and respiration at the expense of $\text{O}_2/\text{H}_2\text{O}$ —a biogeochemical change in the carbon cycle that greatly ameliorates gradient in alkalinity generated by the biological pump. Together, the percentages calculated from trace element abundances and isotope ratios and biomarker data provide a range of conditions over which to evaluate the platform drowning model.

3 Model setup

We treated carbonate production and dissolution in marine basins with a simple two-box scheme that tracks fluxes of alkalinity (A) and dissolved inorganic carbon (C) following the scheme of Bergmann et al. (2013) and Higgins et al. (2009). In this idealized calculation, the equations for alkalinity balance (A) in the surface (A_1) and deep (A_2) oceans are:

$$\frac{dA_1}{dt} = \frac{1}{V_1} [A_i - 2F_{prod} - F_o\Delta_{alk} + J\nabla A] \quad (3)$$

$$\frac{dA_2}{dt} = \frac{1}{V_2} [2F_{diss} + F_o\Delta_{alk} - J\nabla A] \quad (4)$$

The coupled carbon (C_1 and C_2) equations are:

$$\frac{dC_1}{dt} = \frac{1}{V_1} [C_i - F_{prod} - F_o + J\nabla C] \quad (5)$$

$$\frac{dC_2}{dt} = \frac{1}{V_2} [F_{diss} + F_o - J\nabla C] \quad (6)$$

where V is water volume, F_{prod} is carbonate production in the surface ocean, F_o is organic production in the surface ocean, Δ_{alk} is the alkalinity produced per unit DIC during respiration, ∇ denotes a gradient between the surface and deep oceans, J is the volumetric exchange of water between the surface and deep boxes, and F_{diss} is the dissolution flux of carbonates in the deep oceans. Alkalinity is supplied to seawater by weathering (A_i) and removed by carbonate precipitation (F_{prod}). Some carbonate is dissolved in the deep oceans and porewaters, returning alkalinity to the system (F_{diss}). Carbonate production and dissolution within each box was described by a typical rate law of saturation state, Ω :

$$F_{prod} \propto (\Omega_{surface} - 1)^2 \quad (7)$$

$$F_{diss} \propto (1 - \Omega_{deep})^2 \quad (8)$$

In turn, the average saturation states in each reservoir were taken as a function of alkalinity and dissolved inorganic carbon, which were solved at each step using the solver implemented in CO2sys (Lewis & Wallace, 1998). By charge and/or mass conservation, any process that changes the concentrations of alkalinity and dissolved inorganic carbon in either box will also affect the carbonate precipitation and dissolution fluxes by way of Ω —expressed here as the saturation state of calcite.

Beyond carbonate precipitation and dissolution, we considered two additional processes that transfer alkalinity and carbon between the surface and deep ocean boxes. Physical exchange by advection and/or diffusion (J) transfers alkalinity and DIC according to the gradient, ∇A , between the two boxes. The second transfer mechanism is associated with an advective organic matter flux, F_o (i.e. the sedimentation of biological particles associated with the biological pump as well as omnipresent co-deposition of organic matter associated with fine sediment). Inorganic carbon is consumed in surface waters by photosynthesis and returned at depth through respiration/remineralization. This process also re-distributes alkalinity because metabolic processes either generate or consume alkalinity to a degree based on the identity of the participating redox pair. Rather than track individual redox species, we use the net ratios of DIC:alkalinity change, Δ_{alk} , balanced for typical marine organic matter by Bergmann et al. (2013).

4 Results

Using modern ocean basins as a starting point, the model was used to investigate the effects of changing Δ_{alk} on patterns of carbonate precipitation and dissolution. The default steady state is characterized by $\Delta_{alk} = 0$ (well-oxygenated seawater) and by setting the carbonate flux out of the surface ocean, F_c , to its modern value of four times the weathering flux, A_i . We then approximated an OAE using a 200 ky period of reduced oxygen availability ($\Delta_{alk} = 0.6$) with 50 ky onset and recovery periods (Fig. 2a). Rather than capturing the entire complexity of OAEs, dimensionalizing the model in this way couples the carbonate system to known redox changes over timescales empirically derived from observations of the sedimentary record (>100ky). After the 50 ky transition interval, the carbonate system settled into a new steady state that persisted until Δ_{alk}

243 changes again. As expected, the new steady state during the nadir of the OAE was char-
244 acterized by lower Ω and lower rates of carbonate production in the surface ocean (Fig.
245 2b,c).

246 At timescales of >10 ky, disturbances associated with the simulated OAE could be
247 approximated as quasi-steady changes. Plotting steady state solutions as functions of
248 Δ_{alk} related changes in carbonate production and dissolution to the extent of anoxia given
249 reasonable simplifying assumptions. First, we considered a simplified case of two redox
250 pairs $\text{O}_2/\text{H}_2\text{O}$ ($\Delta_{alk} = 0$) and $\text{H}_2\text{S}/\text{SO}_4$ ($\Delta_{alk} = 1.2$)—so that the horizontal axis rep-
251 resents a weighted mixture between the two Δ_{alk} vectors. If the percentage of aerobic
252 respiration replaced by sulfate reduction is roughly analogous to the percentage of the
253 seafloor covered by anoxic bottom waters, then the maximum Δ_{alk} value can be estimated
254 from studies of redox-sensitive elements and biomarkers for photic zone euxinia (Section
255 2.2). Second, we assumed that the sedimentation rate for shallow-water platforms closely
256 follows the overproduction of the surface ocean rather than globally-averaged carbon-
257 ate burial, (F_{prod}), which seems reasonable based on modern estimates of global accu-
258 mulation rates (e.g., Milliman & Droxler, 1996), which is the same among all valid steady
259 state solutions. Under these assumptions, carbonate accumulation on platforms decreases
260 with the spread of ocean anoxia, presenting a plausible mechanism for platform drown-
261 ing.

262 5 Discussion

263 5.1 Redox changes as a drowning mechanism during OAE2

264 The simple model presented above suggests that large scale redox changes in ma-
265 rine basins can provide a reasonable drowning mechanism for carbonate platforms. Re-
266 sults revealed that carbonate production is a non-linear function of these redox changes;
267 the shape of this function indicated that significant decreases in carbonate sedimenta-
268 tion can occur during even modest expansion of anoxia (Fig. 2d). For OAE2, the concave-
269 up response is important because estimates of peak anoxic conditions vary widely among
270 proxies. While the lowest estimates of seafloor anoxia during this interval (1-2, % Montoya-
271 Pino et al., 2010) would produce a very small response, a maximum extent of only 15%
272 (Clarkson et al., 2018) would reduce carbonate sedimentation to 82% of its initial value.
273 For proxy records that suggest 40-50% seafloor anoxia during OAE2 (Monteiro et al.,
274 2012; Ostrander et al., 2017), carbonate sedimentation rates would fall precipitously to
275 approximately half of their original values.

276 Another important aspect of the model results is the timescales of the processes
277 involved. When Δ_{alk} is perturbed, negative feedbacks push the systems towards a new
278 steady state, allowing lower sedimentation rates to be sustained over arbitrarily long timescales
279 (Fig. 3a-c). The estimated timescale for OAE2 is between 250 and 885 kyr (Kolonic et
280 al., 2005; Sageman et al., 2006), and some evidence suggests that the proto-Atlantic was
281 partially anoxic before the event (Monteiro et al., 2012). Taken together, these results
282 suggest that redox changes associated with OAEs could reduce carbonate sedimentation
283 rates on carbonate platforms for $>10^5$ years. As discussed by Schlager (1999), drown-
284 ing requires not only short-term stresses but also longer-term 'environmental deteriora-
285 tion' because carbonate accumulation rates are closely matched with thermal subsidence
286 (<1 order of magnitude) over timescales of 10^5 - 10^6 years. In this context, a redox-based
287 drowning mechanism provides a background stress that connects shorter-term environ-
288 mental collapse (e.g., ocean acidification) with drowning due to long-term tectonic sub-
289 sidence.

290 The shallow-water record for OAE2 shows a variety of carbonate platform responses
291 consistent with the mechanisms outlined here. Platform drowning during and immedi-
292 ately after OAE2 has been documented in the Pyrenees (Drzewiecki & Simo, 2000), the

293 Adriatic platform (Korbar et al., 2012), and the southern Gulf of Mexico (Elrick et al.,
294 2009). In the aforementioned cases, comparisons between geochemical and stratigraphic
295 records suggested that drowning was related to OAE2, but the onset and termination
296 of drowning varied among sections. Results for the idealized cases shown in Figure 2 de-
297 picted an average case for a global change in redox chemistry in ocean basins, but we
298 recognized that patterns of carbonate accumulation in sedimentary basins also reflects
299 an interplay between sedimentation and locally and/or regionally varying degrees of ac-
300 commodation; and the extent to which OAE2 was characterized by platform drowning
301 depended also on the tectonic setting. For example, platforms in the central Tethys (e.g.,
302 the Apulia Platform) experienced uplift and karstification near the Cenomanian-Turonian
303 boundary, and these changes in basin development were locally more important than OAE2
304 in shaping platform stratigraphy (Bosellini et al., 1999). In short, a redox-drowning mech-
305 anism does not necessarily imply perfect synchronicity between the onset of carbon cy-
306 cle and redox changes (e.g. evidenced by isotope excursions) and transgression, because
307 some inherent variability in drowning patterns is to be expected due to regional tecton-
308 ics.

309 The model presented here is idealized, and there are additional considerations when
310 comparing it to the complexity of OAEs in the stratigraphic record. While platform drown-
311 ing at OAEs is particularly common, it is not ubiquitous as some platforms experienced
312 incipient drowning followed by rapid recovery (Parente et al., 2007) and yet others dis-
313 played little evidence of drowning at all (Navarro-Ramirez et al., 2016). An obvious sim-
314 plification is that we treat the surface oceans as a single, well-mixed reservoir and do not
315 consider the sorts of spatial variability in carbonate production and dissolution that re-
316 sult from climate and oceanographic factors. Patterns of carbonate dissolution in the mod-
317 ern oceans vary based on regional variations in temperature and circulation patterns and
318 the strength of the biological pump (Archer, 1996). It is highly likely that ancient ma-
319 rine basins displayed similar heterogeneities, but the geological observables involving the
320 degree of anoxia and pathways of ocean circulation and primary production is not suf-
321 ficiently well-resolved spatially to support breaking up the model domains to more re-
322 alistically simulate local or regional patterns in carbonate sedimentation. As this type
323 of data is generated by future studies the redox-drowning model provides a testable hy-
324 pothesis regarding local variations in platform drowning (Fig. 1a) and anoxia in the ad-
325 jacent ocean basin.

326 5.2 Comparison with other drowning mechanisms

327 The redox-drowning mechanism has several interesting features that contrast with
328 nutrient drowning and acidification-overshoot mechanisms. Numerical models of acidification-
329 overshoot scenarios show that low Ω conditions decay in <100 ky because carbonate com-
330 pensation and silicate weathering feedbacks operate to mitigate the perturbation over
331 relatively short timescales (Archer et al., 1997; Hönisch et al., 2012; Knoll et al., 2011;
332 Payne & Kump, 2007). Short-term acidification is followed by an alkalinity ‘overshoot’
333 where high Ω conditions prevail, which can help the platform recover and presents an
334 impediment to sustained drowning. Reduced carbonate production under a redox drown-
335 ing scenario instead labors over longer characteristic timescales related to the drivers of
336 sustained anoxia; geological observations indicate that these anoxic events can last up
337 to 1 My (Y.-X. Li et al., 2008), akin to the timescales associated with Earth’s atmospheric
338 dioxygen budget in terms of organic carbon burial. In this redox-drowning model there
339 need not be any alkalinity overshoot and drowning can proceed over long timescales with
340 ongoing basin subsidence.

341 The redox-drowning model has indirect overlap with the nutrient-drowning hypoth-
342 esis since many interpretations of OAEs favor increased nutrients and primary produc-
343 tivity as the driver of anoxia (Jenkyns, 2010). However, a key difference is that the rate
344 laws used in the model (Eqns. 7-8) are not specific to the animal and algal taxa that might

345 important for a particular carbonate factory—and while there may be real differences
346 related to biological turnover and changes in the abundance and ecology of marine cal-
347 cifiers during these events, that the dynamics can be generalized within a common car-
348 bonate precipitation rate law suggests that the results hold for a variety of skeletal and
349 non-skeletal facies. This generality complements the nutrient-drowning hypothesis, which
350 was calibrated to modern calcifying taxa and thus assumes that the dominant sediment
351 producers are phototrophic organisms (Hallock & Schlager, 1986). Reduced sedimenta-
352 tion rates should apply to heterotrophic sediment producers (e.g., crinoids) and micro-
353 bial build-ups, both of which are common in drowning successions (Ettinger et al., 2020;
354 Huck et al., 2010; Föllmi et al., 1994). One limitation of our model is that we grouped
355 carbonate produced in the surface oceans as a singular pool and did not distinguish among
356 pelagic, photozoan, heterozoan, and microbial modes of carbonate production. While
357 this simplification generalizes the model, it does not account for the possibility that re-
358 duced carbonate production may not have been evenly distributed among these facto-
359 ries. Several studies have advanced the notion that expansion of microbial (Huck et al.,
360 2010) and heterozoan (Föllmi et al., 2006) carbonate factories could partially compen-
361 sate for reduced photozoan sedimentation, and mechanistic treatment of these factors
362 and potential carbonate sedimentation tradeoffs may be useful in the future.

363 The redox-drowning model does not exclude other drowning scenarios (Godet, 2013),
364 and it may have acted in conjunction with nutrient drowning and acidification-overshoot
365 mechanisms. It is likely that local stratigraphic records show a combined drowning sig-
366 nal that depends on the relative strength and timescales of individual mechanisms (Fig.
367 3). Composite drowning scenarios may explain the diversity of patterns seen in the ge-
368 ologic record including ‘pulsed’ drowning events (e.g., Krencker et al., 2020).

369 5.3 Redox drowning and other anoxic episodes

370 The most important assumption of the redox drowning model is that, like today,
371 the surface oceans were characterized by an overproduction of carbonate. The applica-
372 bility of redox drowning—both for OAEs and for other anoxic episodes—depends on why
373 the surface ocean overproduces carbonate as well as how overproduction has changed through
374 time. At least two factors might have changed carbonate overproduction in the past: an-
375 imal evolution and dioxygen availability. The evolutionary factor involves a Jurassic ra-
376 diation of pelagic calcifying organisms—the primary sources of carbonate sediment fluxes
377 into the deep oceans—in an event known as the mid-Mesozoic Revolution (e.g., Ridg-
378 well, 2005).

379 Prior to this time, marine carbonate production was largely restricted to the con-
380 tinental shelves (i.e., carbonate platforms), limiting carbonate flux across the lysocline.
381 In several previous models of Phanerozoic carbonate chemistry (e.g., Zeebe & Westbroek,
382 2003; Ridgwell, 2005), the mid-Mesozoic Revolution represents the onset of significant
383 carbonate dissolution in deep marine basins, and thus carbonate overproduction is nec-
384 essary to balance the alkalinity budget (Eqn. 2). Since we observed in the redox drown-
385 ing model that the amount of change in carbonate sedimentation patterns is largest when
386 the initial overproduction is high, this mechanism should be particularly applicable to
387 conditions attained in the latter part of Phanerozoic time, and may even post-date the
388 Toarcian OAE (Jenkyns, 2010). A evolutionary trend toward carbonate overproduction
389 would emphasize similarities between Cretaceous OAEs, the PETM, and early Cenozoic
390 hyperthermal events—but might differentiate these from earlier anoxic episodes such as
391 the Toarcian OAE and the end-Permian extinction.

392 Nevertheless, the role of the biological pump underpinned by oxygenic photosyn-
393 thesis and aerobic respiration in carbonate dissolution suggests that the condition of car-
394 bonate overproduction in the surface oceans may be substantially more ancient (Higgins
395 et al., 2009; Knoll et al., 2016). Carbonate dissolution is not limited to the deep ocean

396 as aerobic respiration can drive significant dissolution above the lysocline (Milliman et
 397 al., 1999) and near-surface porewaters dissolve carbonate even in platform-top settings
 398 (Walter & Burton, 1990). These observations point to at least some degree of carbon-
 399 ate overproduction prior to mid-Mesozoic time and suggest that redox drowning might
 400 have affected carbonate platforms during Paleozoic and early Mesozoic anoxic episodes.
 401 The potential sensitivity of carbonate production and stratigraphy to changes in the re-
 402 dox structure of marine basins should motivate further efforts in the comparative sed-
 403 imentology of drowning events; similarities or differences in the stratigraphic records may
 404 reveal much about how the Earth system's response to cycle perturbations has changed
 405 through time due to evolutionary and biogeochemical trends.

406 Data and Acknowledgements

407 The model as described in the main text and SI is available through a Github repos-
 408 itory (www.doi.org/10.5281/zenodo.4549245). B. Smith acknowledges support from the
 409 Agouron Institute Postdoctoral Fellowship, C. Kerans acknowledges support from the
 410 Reservoir Characterization Research Lab, and W. Fischer acknowledges support from
 411 the Caltechs Rothberg Innovative Initiative and the Caltech Center for Evolutionary Sci-
 412 ence. The authors are not aware of any conflicts of interest.

413 References

- 414 Amante, C., & Eakins, B. W. (n.d.). *Volumes of the World's Oceans from ETOPO1*.
 415 (data retrieved from NOAA, [https://www.ngdc.noaa.gov/mgg/global/
 416 etopo1_ocean_volumes.html](https://www.ngdc.noaa.gov/mgg/global/etopo1_ocean_volumes.html))
- 417 Archer, D. E. (1996). An atlas of the distribution of calcium carbonate in sediments
 418 of the deep sea. *Global Biogeochemical Cycles*, *10*(1), 159–174.
- 419 Archer, D. E., Kheshgi, H., & Maier-Reimer, E. (1997). Multiple timescales for neu-
 420 tralization of fossil fuel CO₂. *Geophysical Research Letters*, *24*(4), 405–408.
- 421 Arthur, M., & Schlanger, S. (1979). Cretaceous Oceanic Anoxic Events as causal fac-
 422 tors in development of reef-reservoired giant oil fields. *AAPG bulletin*, *63*(6),
 423 870–885.
- 424 Arthur, M., Schlanger, S. t., & Jenkyns, H. (1987). The Cenomanian-Turonian
 425 Oceanic Anoxic Event, ii. palaeoceanographic controls on organic-matter pro-
 426 duction and preservation. *Geological Society, London, Special Publications*,
 427 *26*(1), 401–420.
- 428 Baud, A., Richoz, S., & Pruss, S. (2007). The lower Triassic anachronistic carbonate
 429 facies in space and time. *Global and Planetary Change*, *55*(1-3), 81–89.
- 430 Beatty, T. W., Zonneveld, J., & Henderson, C. M. (2008). Anomalously diverse
 431 early triassic ichnofossil assemblages in northwest pangea: a case for a shallow-
 432 marine habitable zone. *Geology*, *36*(10), 771–774.
- 433 Bergmann, K. D., Grotzinger, J. P., & Fischer, W. W. (2013). Biological influences
 434 on seafloor carbonate precipitation. *Palaios*, *28*(2), 99–115.
- 435 Blättler, C. L., Jenkyns, H. C., Reynard, L. M., & Henderson, G. M. (2011). Sig-
 436 nificant increases in global weathering during Oceanic Anoxic Events 1a and 2
 437 indicated by calcium isotopes. *Earth and Planetary Science Letters*, *309*(1-2),
 438 77–88.
- 439 Bosellini, A., Morsilli, M., & Neri, C. (1999). Long-term event stratigraphy of the
 440 apulia platform margin (upper jurassic to eocene, gargano, southern italy).
 441 *Journal of Sedimentary Research*, *69*(6), 1241–1252.
- 442 Broecker, W. S. (1998). *Greenhouse puzzles: Keeling's world, Martin's world,
 443 Walker's world*. Eldigio Press.
- 444 Broecker, W. S., & Peng, T.-H. (1982). *Tracers in the sea*. Lamont-Doherty Geolog-
 445 ical Observatory, Columbia University Palisades, New York.

- 446 Clarkson, M. O., Stirling, C. H., Jenkyns, H. C., Dickson, A. J., Porcelli, D., Moy,
447 C. M., ... Lenton, T. M. (2018). Uranium isotope evidence for two episodes
448 of deoxygenation during Oceanic Anoxic Event 2. *Proceedings of the National
449 Academy of Sciences*, 115(12), 2918–2923.
- 450 Damsté, J. S. S., & Köster, J. (1998). A euxinic southern North Atlantic Ocean
451 during the Cenomanian/Turonian Oceanic Anoxic Event. *Earth and Planetary
452 Science Letters*, 158(3-4), 165–173.
- 453 Drzewiecki, P. A., & Simo, J. T. (2000). Tectonic, eustatic and environmental controls
454 on mid-cretaceous carbonate platform deposition, south-central Pyrenees,
455 Spain. *Sedimentology*, 47(3), 471–495.
- 456 Dunne, J. P., Hales, B., & Toggweiler, J. (2012). Global calcite cycling constrained
457 by sediment preservation controls. *Global Biogeochemical Cycles*, 26(3).
- 458 Elrick, M., Molina-Garza, R., Duncan, R., & Snow, L. (2009). C-isotope stratig-
459 raphy and paleoenvironmental changes across oae2 (mid-cretaceous) from
460 shallow-water platform carbonates of southern Mexico. *Earth and Planetary
461 Science Letters*, 277(3-4), 295–306.
- 462 Ettinger, N. P., Larson, T. E., Kerans, C., Thibodeau, A. M., Hattori, K. E., Kacur,
463 S. M., & Martindale, R. C. (2020). Ocean acidification and photic-zone anoxia
464 at the Toarcian Oceanic Anoxic Event: Insights from the Adriatic Carbonate
465 Platform. *Sedimentology*.
- 466 Föllmi, K. B., Godet, A., Bodin, S., & Linder, P. (2006). Interactions between
467 environmental change and shallow water carbonate buildup along the north-
468 ern Tethyan margin and their impact on the Early Cretaceous carbon isotope
469 record. *Paleoceanography*, 21(4).
- 470 Föllmi, K. B., Weissert, H., Bisping, M., & Funk, H. (1994). Phosphogenesis,
471 carbon-isotope stratigraphy, and carbonate-platform evolution along the lower
472 cretaceous northern Tethyan margin. *Geological Society of America Bulletin*,
473 106(6), 729–746.
- 474 Forster, A., Kuypers, M. M., Turgeon, S. C., Brumsack, H.-J., Petrizzo, M. R., &
475 Damsté, J. S. S. (2008). The Cenomanian/Turonian Oceanic Anoxic Event
476 in the South Atlantic: New insights from a geochemical study of DSDP site
477 530A. *Palaeogeography, Palaeoclimatology, Palaeoecology*, 267(3-4), 256–283.
- 478 Franceschi, M., Preto, N., Marangon, A., Gattolin, G., & Meda, M. (2016). High
479 precipitation rate in a Middle Triassic carbonate platform: Implications on
480 the relationship between seawater saturation state and carbonate production.
481 *Earth and Planetary Science Letters*, 444, 215–224.
- 482 Gattuso, J.-P., Epitalon, J.-M., Lavigne, H., & Orr, J. (2019). seacarb: Seawater
483 carbonate chemistry. R package version 3.2. 12.
- 484 Godet, A. (2013). Drowning unconformities: Palaeoenvironmental significance and
485 involvement of global processes. *Sedimentary Geology*, 293, 45–66.
- 486 Grotzinger, J. P., & Knoll, A. H. (1995). Anomalous carbonate precipitates; is the
487 Precambrian the key to the Permian? *Palaios*, 10(6), 578–596.
- 488 Hales, B. (2003). Respiration, dissolution, and the lysocline. *Paleoceanography*,
489 18(4).
- 490 Hallock, P., & Schlager, W. (1986). Nutrient excess and the demise of coral reefs
491 and carbonate platforms. *Palaios*, 1(4), 389–398.
- 492 Heldt, M., Lehmann, J., Bachmann, M., Negra, H., & Kuss, J. (2010). Increased
493 terrigenous influx but no drowning: palaeoenvironmental evolution of the
494 Tunisian carbonate platform margin during the Late Aptian. *Sedimentology*,
495 57(2), 695–719.
- 496 Helly, J. J., & Levin, L. A. (2004). Global distribution of naturally occurring marine
497 hypoxia on continental margins. *Deep Sea Research Part I: Oceanographic Re-
498 search Papers*, 51(9), 1159–1168.
- 499 Higgins, J. A., Fischer, W., & Schrag, D. (2009). Oxygenation of the ocean and sed-
500 iments: consequences for the seafloor carbonate factory. *Earth and Planetary*

- 501 *Science Letters*, 284(1-2), 25–33.
- 502 Hoffman, P. F., Abbot, D. S., Ashkenazy, Y., Benn, D. I., Brocks, J. J., Cohen,
503 P. A., ... others (2017). Snowball Earth climate dynamics and Cryogenian
504 geology-geobiology. *Science Advances*, 3(11), e1600983.
- 505 Hoffman, P. F., Kaufman, A. J., Halverson, G. P., & Schrag, D. P. (1998). A Neo-
506 proterozoic snowball earth. *Science*, 281(5381), 1342–1346.
- 507 Hönisch, B., Ridgwell, A., Schmidt, D. N., Thomas, E., Gibbs, S. J., Sluijs, A., ...
508 others (2012). The geological record of ocean acidification. *Science*, 335(6072),
509 1058–1063.
- 510 Huck, S., Rameil, N., Korbar, T., Heimhofer, U., Wiczorek, T. D., & Immenhauser,
511 A. (2010). Latitudinally different responses of tethyan shoal-water carbonate
512 systems to the Early Aptian Oceanic Anoxic Event (OAE 1a). *Sedimentology*,
513 57(7), 1585–1614.
- 514 Jenkyns, H. (2010). Geochemistry of oceanic anoxic events. *Geochemistry, Geo-*
515 *physics, Geosystems*, 11(3).
- 516 Kelley, B. M., Daniel, L. J., Yu, M., Jost, A. B., Meyer, K. M., Lau, K. V., ... oth-
517 ers (2020). Controls on carbonate platform architecture and reef recovery
518 across the Palaeozoic to Mesozoic transition: A high-resolution analysis of the
519 Great Bank of Guizhou. *Sedimentology*, 67(6), 31193151.
- 520 Kiessling, W., & Simpson, C. (2011). On the potential for ocean acidification to be a
521 general cause of ancient reef crises. *Global Change Biology*, 17(1), 56–67.
- 522 Knoll, A. H., Bergmann, K. D., & Strauss, J. V. (2016). Life: the first two billion
523 years. *Philosophical Transactions of the Royal Society B: Biological Sciences*,
524 371(1707), 20150493.
- 525 Knoll, A. H., Fischer, W. W., Gattuso, J., & Hansson, L. (2011). Skeletons and
526 ocean chemistry: the long view. *Ocean Acidification*, 4, 67–82.
- 527 Kolonic, S., Wagner, T., Forster, A., Sinninghe Damsté, J. S., Walsworth-Bell, B.,
528 Erba, E., ... others (2005). Black shale deposition on the northwest African
529 Shelf during the Cenomanian/Turonian oceanic anoxic event: Climate coupling
530 and global organic carbon burial. *Paleoceanography*, 20(1).
- 531 Korbar, T., Glumac, B., Tešović, B. C., & Cadieux, S. B. (2012). Response of a car-
532 bonate platform to the cenomanian–turonian drowning and oae 2: a case study
533 from the adriatic platform (dalmatia, croatia) carbonate platform response
534 to the cenomanian–turonian drowning and oae 2. *Journal of Sedimentary*
535 *Research*, 82(3), 163–176.
- 536 Krencker, F.-N., Fantasia, A., Danisch, J., Martindale, R., Kabiri, L., El Ouali, M.,
537 & Bodin, S. (2020). Two-phased collapse of the shallow-water carbonate
538 factory during the late Pliensbachian–Toarcian driven by changing climate
539 and enhanced continental weathering in the Northwestern Gondwana Margin.
540 *Earth-Science Reviews*, 103254.
- 541 Kuypers, M. M., Pancost, R. D., Nijenhuis, I. A., & Sinninghe Damsté, J. S. (2002).
542 Enhanced productivity led to increased organic carbon burial in the euxinic
543 North Atlantic basin during the late Cenomanian Oceanic Anoxic Events.
544 *Paleoceanography*, 17(4), 3–1.
- 545 Lasaga, A. C., Berner, R. A., & Garrels, R. M. (1985). An improved geochemical
546 model of atmospheric CO₂ fluctuations over the past 100 million years. *The*
547 *carbon cycle and atmospheric CO₂: natural variations Archean to present*, 32,
548 397–411.
- 549 Laya, J. C., Albader, A., Kaczmarek, S., Pope, M., Harris, P. M., & Miller, B.
550 (2021). Dissolution of ooids in seawater-derived fluids—an example from lower
551 permian re-sedimented carbonates, west texas, usa. *Sedimentology*.
- 552 Lechler, M., von Strandmann, P. A. P., Jenkyns, H. C., Prosser, G., & Parente,
553 M. (2015). Lithium-isotope evidence for enhanced silicate weathering during
554 OAE 1a (Early Aptian Selli event). *Earth and Planetary Science Letters*, 432,
555 210–222.

- 556 Lehrmann, D. J., Bentz, J. M., Wood, T., Goers, A., Dhillon, R., Akin, S., . . . oth-
 557 ers (2015). Environmental controls on the genesis of marine microbialites
 558 and dissolution surface associated with the end-Permian mass extinction: new
 559 sections and observations from the Nanpanjiang Basin, South China. *Palaios*,
 560 *30*(7), 529–552.
- 561 Lewis, E., & Wallace, D. (1998). *Program developed for CO₂ system calculations*
 562 (Tech. Rep.). Environmental System Science Data Infrastructure for a Virtual
 563 Ecosystem.
- 564 Li, Y.-H., Takahashi, T., & Broecker, W. S. (1969). Degree of saturation of CaCO₃
 565 in the oceans. *Journal of Geophysical Research*, *74*(23), 5507–5525.
- 566 Li, Y.-X., Bralower, T. J., Montañez, I. P., Osleger, D. A., Arthur, M. A., Bice,
 567 D. M., . . . Silva, I. P. (2008). Toward an orbital chronology for the early
 568 aptian oceanic anoxic event (oae1a, ~ 120 ma). *Earth and Planetary Science*
 569 *Letters*, *271*(1-4), 88–100.
- 570 Lueker, T. J., Dickson, A. G., & Keeling, C. D. (2000). Ocean pCO₂ calculated from
 571 dissolved inorganic carbon, alkalinity, and equations for K1 and K2: validation
 572 based on laboratory measurements of CO₂ in gas and seawater at equilibrium.
 573 *Marine chemistry*, *70*(1-3), 105–119.
- 574 Melim, L., Westphal, H., Swart, P., Eberli, G., & Munnecke, A. (2002). Questioning
 575 carbonate diagenetic paradigms: evidence from the Neogene of the Bahamas.
 576 *Marine Geology*, *185*(1-2), 27–53.
- 577 Millero, F. J. (1995). Thermodynamics of the carbon dioxide system in the oceans.
 578 *Geochimica et Cosmochimica Acta*, *59*(4), 661–677.
- 579 Milliman, J., & Droxler, A. (1996). Neritic and pelagic carbonate sedimentation in
 580 the marine environment: ignorance is not bliss. *Geologische Rundschau*, *85*(3),
 581 496–504.
- 582 Monteiro, F., Pancost, R., Ridgwell, A., & Donnadieu, Y. (2012). Nutrients as the
 583 dominant control on the spread of anoxia and euxinia across the Cenomanian-
 584 Turonian Oceanic Anoxic Event (OAE2): Model-data comparison. *Paleo-*
 585 *ceanography*, *27*(4).
- 586 Montoya-Pino, C., Weyer, S., Anbar, A. D., Pross, J., Oschmann, W., van de
 587 Schootbrugge, B., & Arz, H. W. (2010). Global enhancement of ocean anoxia
 588 during Oceanic Anoxic Event 2: A quantitative approach using U isotopes.
 589 *Geology*, *38*(4), 315–318.
- 590 Munhoven, G. (2002). Glacial-interglacial changes of continental weathering: es-
 591 timates of the related CO₂ and HCO₃⁻ flux variations and their uncertainties.
 592 *Global and Planetary Change*, *33*(1-2), 155–176.
- 593 Navarro-Ramirez, J. P., Bodin, S., & Immenhauser, A. (2016). Ongoing cenoma-
 594 nianturonian heterozoan carbonate production in the neritic settings of peru.
 595 *Sedimentary Geology*, *331*, 78–93.
- 596 Ostrander, C. M., Owens, J. D., & Nielsen, S. G. (2017). Constraining the rate
 597 of oceanic deoxygenation leading up to a Cretaceous Oceanic Anoxic Event
 598 (OAE-2: ~ 94 ma). *Science advances*, *3*(8), e1701020.
- 599 Pancost, R. D., Crawford, N., Magness, S., Turner, A., Jenkyns, H. C., & Maxwell,
 600 J. R. (2004). Further evidence for the development of photic-zone euxinic
 601 conditions during Mesozoic Oceanic Anoxic Event. *Journal of the Geological*
 602 *Society*, *161*(3), 353–364.
- 603 Parente, M., Frijia, G., & Di Lucia, M. (2007). Carbon-isotope stratigraphy of
 604 cenomanian-turonian platform carbonates from the southern apennines (italy):
 605 a chemostratigraphic approach to the problem of correlation between shallow-
 606 water and deep-water successions. *Journal of the Geological Society*, *164*(3),
 607 609–620.
- 608 Payne, J. L., & Kump, L. R. (2007). Evidence for recurrent Early Triassic mas-
 609 sive volcanism from quantitative interpretation of carbon isotope fluctuations.
 610 *Earth and Planetary Science Letters*, *256*(1-2), 264–277.

- 611 Penman, D. E., Turner, S. K., Sexton, P. F., Norris, R. D., Dickson, A. J., Boulila,
612 S., ... others (2016). An abyssal carbonate compensation depth overshoot
613 in the aftermath of the Palaeocene–Eocene Thermal Maximum. *Nature Geo-*
614 *science*, *9*(8), 575–580.
- 615 Phelps, R. M., Kerans, C., Da-Gama, R. O., Jeremiah, J., Hull, D., & Loucks, R. G.
616 (2015). Response and recovery of the Comanche carbonate platform surround-
617 ing multiple Cretaceous Oceanic Anoxic Events, northern Gulf of Mexico.
618 *Cretaceous Research*, *54*, 117–144.
- 619 Phelps, R. M., Kerans, C., Loucks, R. G., Da Gama, R. O., Jeremiah, J., & Hull, D.
620 (2014). Oceanographic and eustatic control of carbonate platform evolution
621 and sequence stratigraphy on the Cretaceous (Valanginian–Campanian) passive
622 margin, northern Gulf of Mexico. *Sedimentology*, *61*(2), 461–496.
- 623 Reinhard, C. T., & Fischer, W. W. (2019). Mechanistic links between the sediment-
624 tary redox cycle and marine acid-base chemistry. *Geochemistry, Geophysics,*
625 *Geosystems*, *20*(12), 5968–5978.
- 626 Ridgwell, A. (2005). A Mid Mesozoic Revolution in the regulation of ocean chem-
627 istry. *Marine Geology*, *217*(3-4), 339–357.
- 628 Sageman, B. B., Meyers, S. R., & Arthur, M. A. (2006). Orbital time scale and
629 new C-isotope record for Cenomanian-Turonian boundary stratotype. *Geology*,
630 *34*(2), 125–128.
- 631 Sarmiento, J. L., & Gruber, N. (2006). *Ocean biogeochemical dynamics*. Princeton
632 University Press.
- 633 Schlager, W. (1981). The paradox of drowned reefs and carbonate platforms. *Geo-*
634 *logical Society of America Bulletin*, *92*(4), 197–211.
- 635 Schlager, W. (1999). Scaling of sedimentation rates and drowning of reefs and car-
636 bonate platforms. *Geology*, *27*(2), 183–186.
- 637 Schlanger, S., & Jenkyns, H. (1976). Cretaceous oceanic anoxic events: Causes and
638 consequences: *Geologie & mijnbouw*, v. 55.
- 639 Scholle, P. A., & Arthur, M. A. (1980). Carbon isotope fluctuations in Cretaceous
640 pelagic limestones: potential stratigraphic and petroleum exploration tool.
641 *AAPG Bulletin*, *64*(1), 67–87.
- 642 Sigman, D. M., & Boyle, E. A. (2000). Glacial/interglacial variations in atmospheric
643 carbon dioxide. *Nature*, *407*(6806), 859–869.
- 644 Trecalli, A., Spangenberg, J., Adatte, T., Föllmi, K. B., & Parente, M. (2012).
645 Carbonate platform evidence of ocean acidification at the onset of the early
646 Toarcian Oceanic Anoxic Event. *Earth and Planetary Science Letters*, *357*,
647 214–225.
- 648 Tziperman, E., Halevy, I., Johnston, D. T., Knoll, A. H., & Schrag, D. P. (2011). Bi-
649 ologically induced initiation of Neoproterozoic snowball-Earth events. *Proceed-*
650 *ings of the National academy of Sciences*, *108*(37), 15091–15096.
- 651 van Buchem, F. S., Al-Husseini, M. I., Maurer, F., Droste, H. J., Yose, L. A., et
652 al. (2010). Sequence-stratigraphic synthesis of the Barremian–Aptian of the
653 eastern Arabian Plate and implications for the petroleum habitat. *Barremian-*
654 *Aptian stratigraphy and hydrocarbon habitat of the eastern Arabian Plate*.
655 *GeoArabia Special Publication*, *4*, 9–48.
- 656 Walker, J. C., Hays, P., & Kasting, J. F. (1981). A negative feedback mechanism for
657 the long-term stabilization of Earth’s surface temperature. *Journal of Geophys-*
658 *ical Research: Oceans*, *86*(C10), 9776–9782.
- 659 Walter, L. M., & Burton, E. A. (1990). Dissolution of recent platform carbonate sed-
660 iments in marine pore fluids. *American Journal of Science*, *290*(6), 601–643.
- 661 Zachos, J. C., Röhl, U., Schellenberg, S. A., Sluijs, A., Hodell, D. A., Kelly, D. C.,
662 ... others (2005). Rapid acidification of the ocean during the Paleocene-
663 Eocene thermal maximum. *Science*, *308*(5728), 1611–1615.
- 664 Zeebe, R. E., & Westbroek, P. (2003). A simple model for the CaCO₃ saturation
665 state of the ocean: The Strangelove, the Neritan, and the Cretan ocean. *Geo-*

666
667
668

chemistry, Geophysics, Geosystems, 4(12).
Zeebe, R. E., & Wolf-Gladrow, D. (2001). *CO₂ in seawater: equilibrium, kinetics, isotopes* (No. 65). Gulf Professional Publishing.

Accepted Article

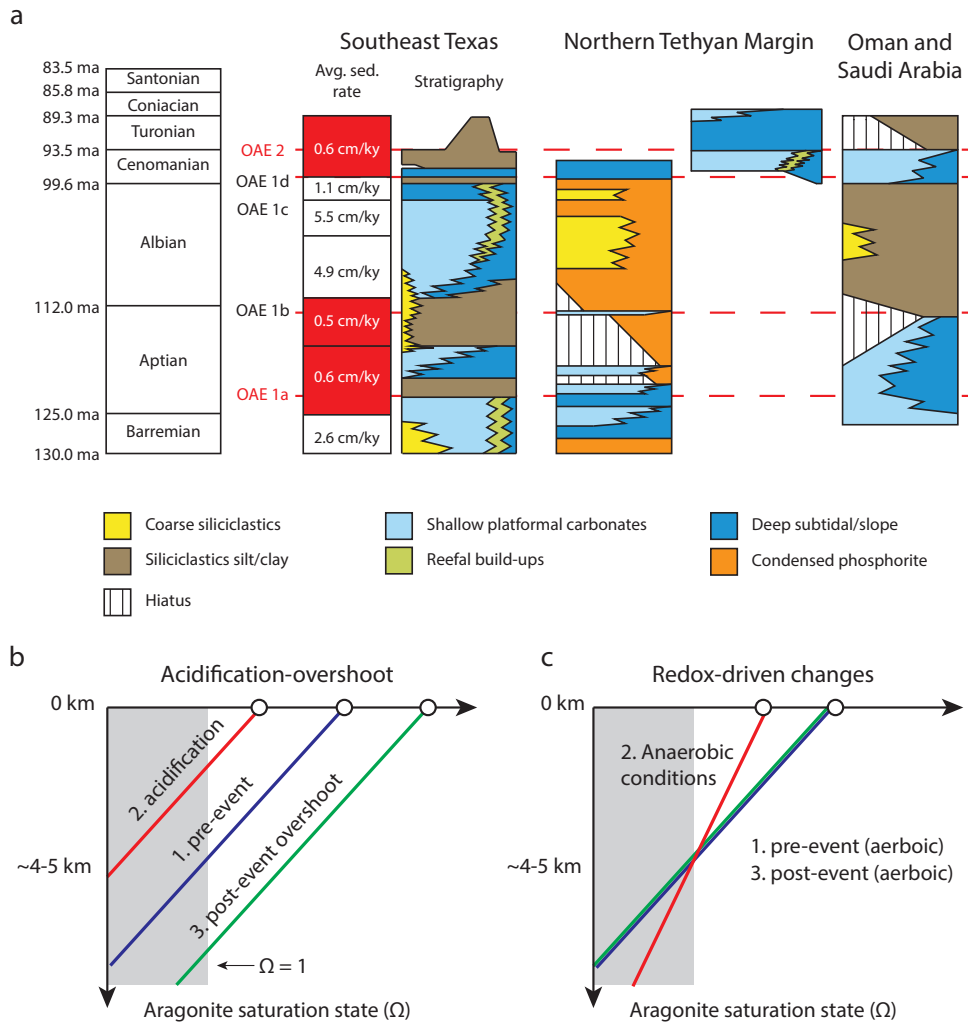


Figure 1. a. Simplified Wheeler diagrams showing stratigraphic patterns of Cretaceous platform drowning for the Texas Gulf Coast Phelps et al. (2014), Northern Tethyan Margin (Föllmi et al., 1994; Föllmi et al., 2006; Drzewiecki & Simo, 2000), and Oman (van Buchem et al., 2010). b,c. Possible effects of OAEs on depth-dependant trends in carbonate saturation state. b. Changes driven by ocean acidification and subsequent recovery of the carbonate system. Under this scenario, CO_2 sourced from volcanic systems or other carbon sources make their way into the atmosphere and oceans, reducing the saturation state and causing the carbonate compensation depth to shallow (red line). Over longer timescales, higher levels of atmospheric CO_2 bring more weathering-derived alkalinity into the oceans. In some cases, additional alkalinity causes the CCD to deepen and ‘overshoot’ its pre-event depth (green line, e.g., Penman et al., 2016). c. Respiration-driven changes in saturation state. Ω gradients (the slopes of the lines) reflect not only on depth-dependant trends in temperature and pressure, but also depend on primary productivity, the strength of the biological pump, and the availability of various electron donor/acceptor pairs. Changes in the availability of oxygen in ocean basins may trigger corresponding changes in the saturation state with depth as various anaerobic metabolisms replace aerobic ones (Higgins et al., 2009; Knoll et al., 2011)

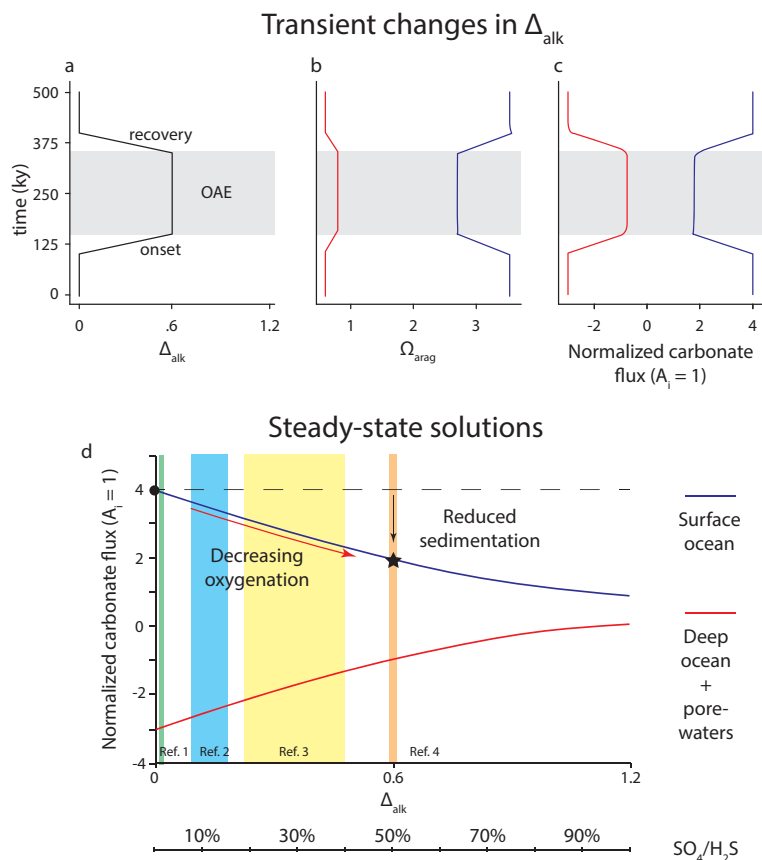


Figure 2. Model response to changes in Δ_{alk} . a. Modeling an OAE as a shift in Δ_{alk} away from aerobic respiration ($\Delta_{alk} = 0$) and towards sulfate reduction ($\Delta_{alk} = 1.2$). The maximum shift, $\Delta_{alk} = 0.6$, is equivalent to 50% of aerobic respiration being replaced by sulfate reduction. b. Changes in Ω caused by changes in Δ_{alk} . As Δ_{alk} increases, deep ocean and porewater Ω is buffered against dissolution at the expense of surface ocean Ω . c. Changes in carbonate fluxes associates with changes in Δ_{alk} . Fluxes are normalized to the alkalinity flux into the ocean, A_i , which is assumed to be constant. The surface ocean curve represents the degree of carbonate overproduction needed to balance out dissolution. As Δ_{alk} approaches increases, the degree of overproduction decreases, which can be interpreted as lower sedimentation rates in shallow water settings. Note that the lowered surface fluxes are a new steady state for the system which persists until Δ_{alk} changes again. References for 1c are 1) Montoya-Pino et al. (2010), 2) Clarkson et al. (2018), 3) Ostrander et al. (2017), and 4) Monteiro et al. (2012).

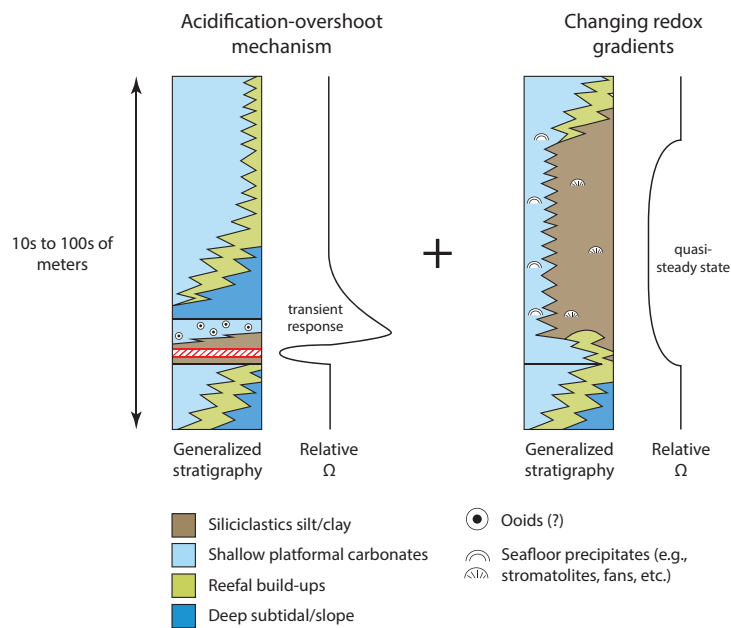


Figure 3. Comparisons between acidification-overshoot and redox-drowning models. The acidification-overshoot model operates over shorter (10-100 ky) timescales. In contrast, the redox-drowning model produces quasi-steady state changes that persist over arbitrarily long timescales. These mechanisms, along with nutrient-driven drowning, are not mutually exclusive; spatial variability and differences in drowning across separate events may be caused by variations in the relative strength of each driver.